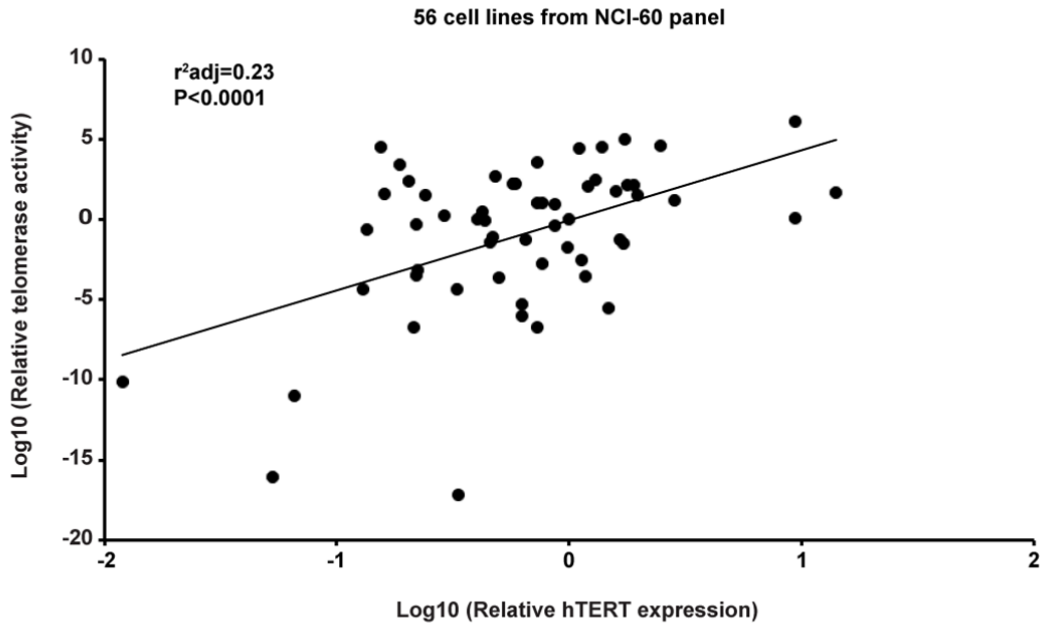


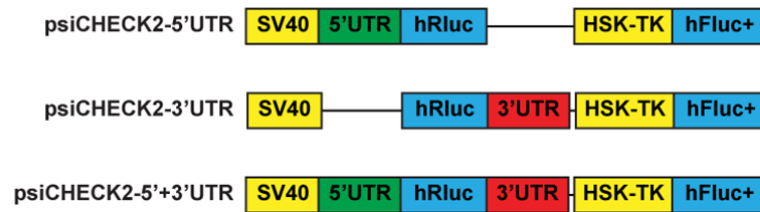
1 **Supplementary Figures**

2

a



b



3

4

5

6 **Supplementary Figure 1: The expression level of *hTERT* mRNA correlates with**  
7 **telomerase activity in cancer cells.**

8 a. Scatter plot for relative telomerase activity and *hTERT* mRNA expression in 56 human  
9 cancer cell lines in NCI-60 panel.

10 b. Schematic representation of the psiCHECK2-3'UTR, psiCHECK2-5'UTR and psiCHECK2-  
11 5'+3'UTR reporter constructs.

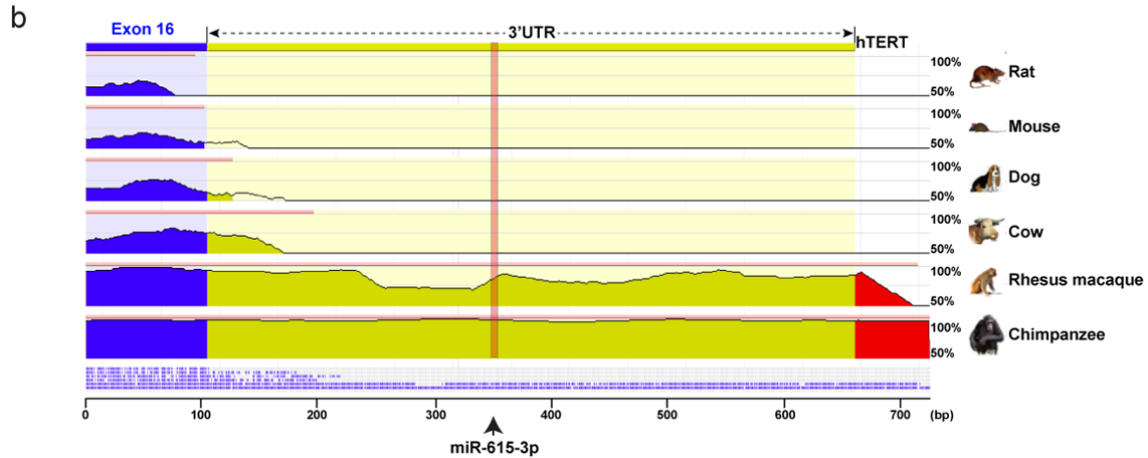
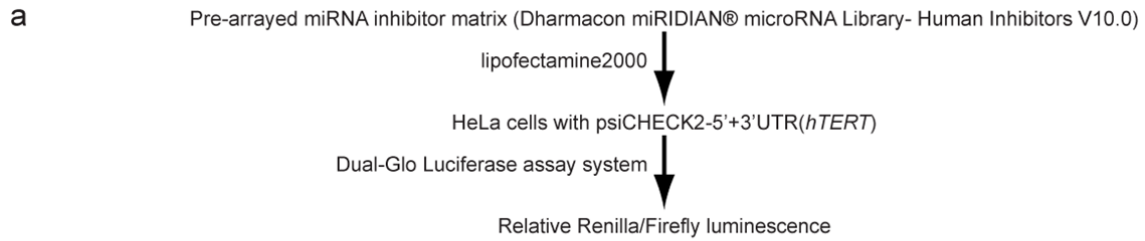
12

13

14

15

16



17

18

19 **Supplementary Figure 2: Genome-wide miRNA inhibitor screen identify miR-615-3p**  
20 **targeting *hTERT* 3'UTR.**

21 a. Design of the genome-wide miRNA inhibitor library screen to identify miRNAs that target  
22 *hTERT* UTRs.

23 b. The 3'UTR sequences of the *TERT* mRNA from rat, mouse, dog, cow, rhesus macaque,  
24 chimpanzee and human were compared using the ECR-Browser software  
25 (<http://ecrbrowser.dcode.org>). The height of the curves (50% < X < 100%) indicates the  
26 homology (blue = exon, yellow = untranslated regions of the RNA, red = intergenic regions,  
27 pink line above indicate evolutionary conserved region). The miR-615-3p target site is  
28 indicated by arrowhead and highlighted in pink.

29

30

31

32

33

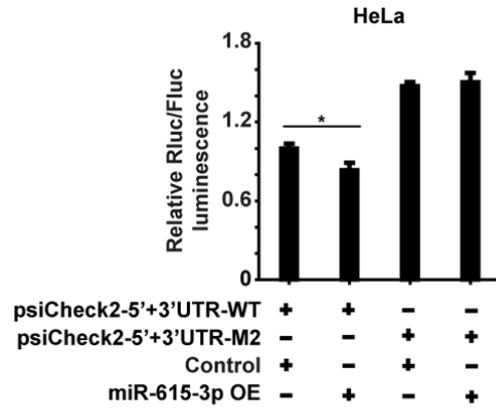
34

35

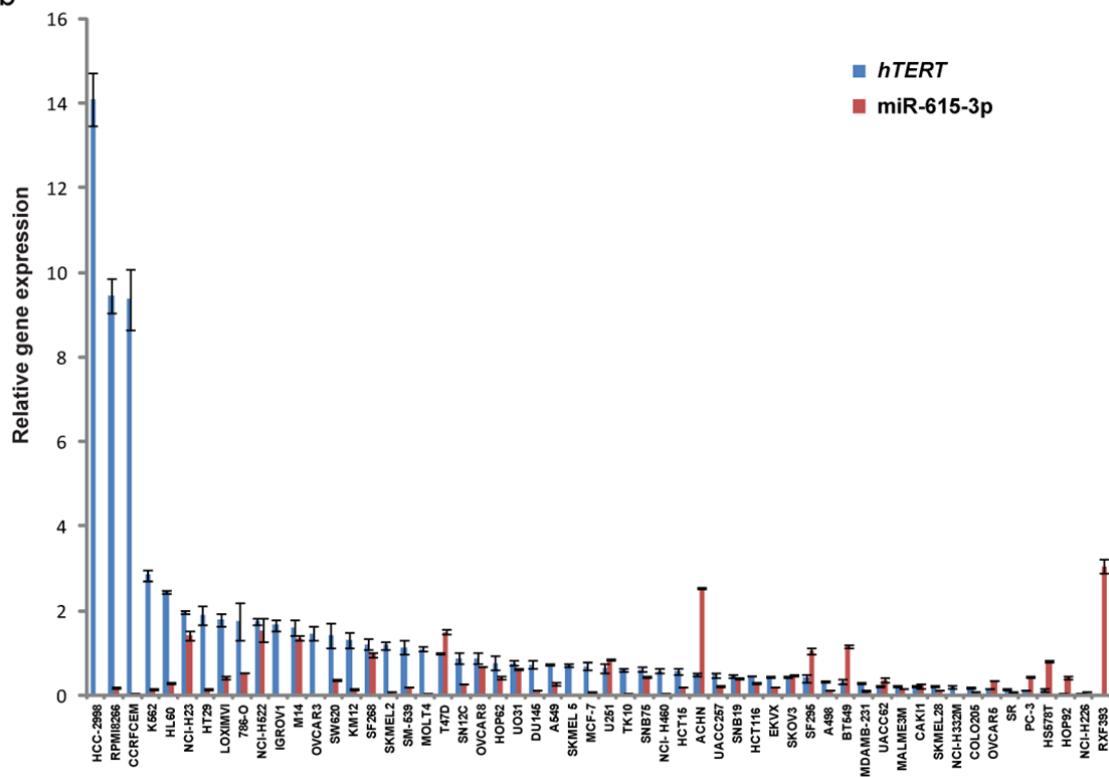
36

37

a



b



38

39 **Supplementary Figure 3: Regulation of *hTERT* expression by miR-615-3p.**

40 a. miR-615-3p targets *hTERT* 3'UTR to suppress *hTERT* expression. Significance was  
 41 determined by t-test. \*  $P \leq 0.05$ .

42 b. The relative expression of *hTERT* mRNA and miR-615-3p in 56 human cancer cell lines in  
 43 NCI-60 panel as quantified by real-time RT-PCR. The expression of *hTERT* mRNA and miR-  
 44 615-3p in 293T cells was set as 1.

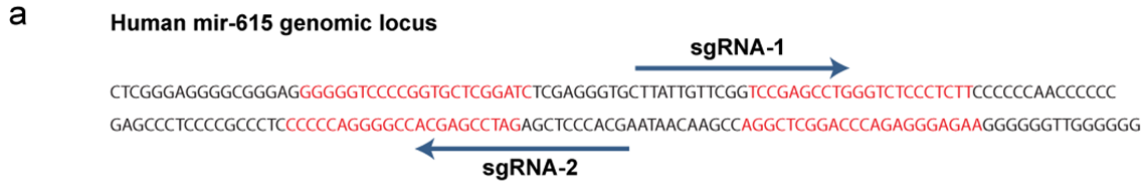
45

46

47

48

49



**Scored by inverse likelihood of off target binding**

Score	Sequence
Guide#1 96	CTTATTGTTTCGGTCCGAGCC TGG
Guide#2 92	CACCCTCGAGATCCGAGCAC CGG

**b RKO mir-615 knockout clone 1 (-15bp,-15bp)**

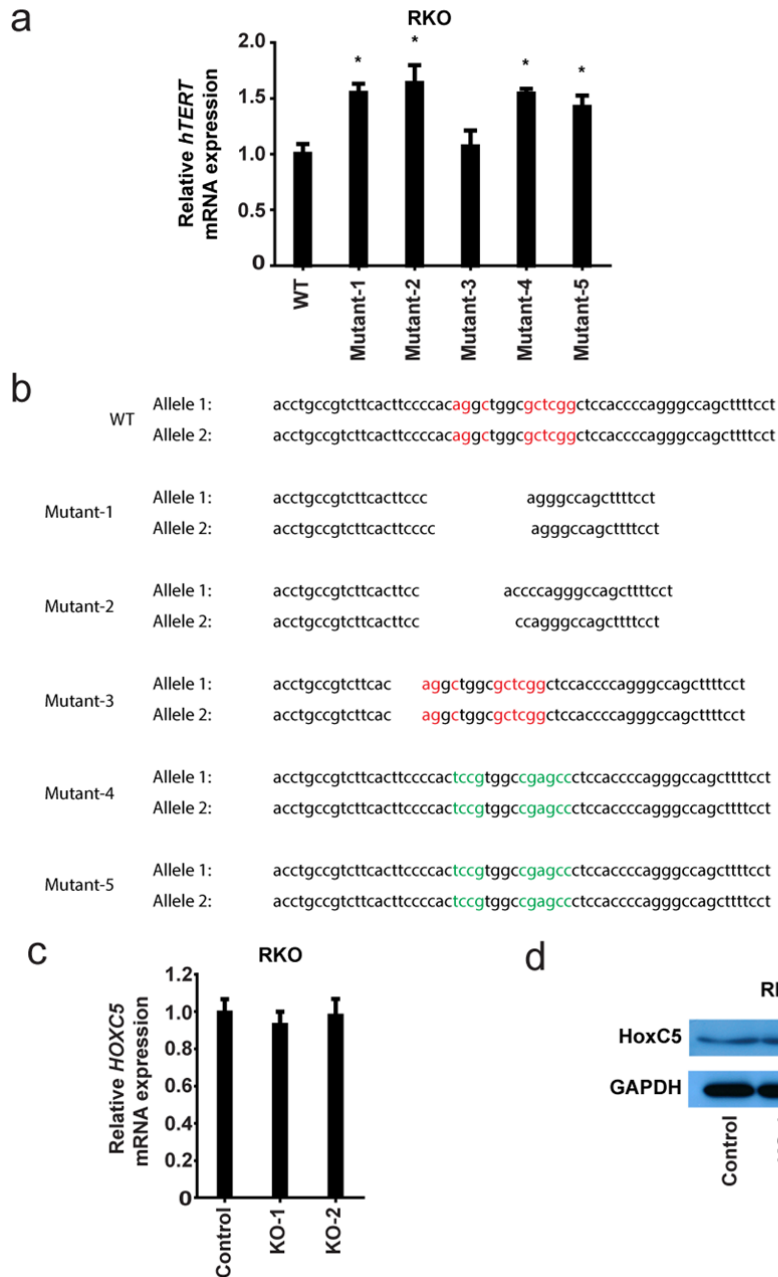
CTCGGAGGGGCGGGAGGGGGTCCCGGTCTCGGATCTCGAGGTGCTTATTGTTTCGGTCCGAGCC GAGCCCTCCCGCCCTCCCCAGGGGCCACGAGCCTAGAGCTCCACGAATAACAAGCCAGGCTCGG	CCGGTCTCGGATCTCGAGGTGCTTATTGTTTCGGTCCGAGCCTGGGTCTCCCTCTTCCCCCAACCCCC GGGGGTTGGGGG
--	--

**RKO mir-615 knockout clone 2 (-5bp,-5bp)**

CTCGGAGGGGCGGGAGGGGG GAGCCCTCCCGCCCTCCCC	CCGGTCTCGGATCTCGAGGTGCTTATTGTTTCGGTCCGAGCCTGGGTCTCCCTCTTCCCCCAACCCCC GCCACGAGCCTAGAGCTCCACGAATAACAAGCCAGGCTCGGACCCAGAGGGAGAAAGGGGGTTGGGGG
---	--

50  
51  
52  
53  
54  
55  
56  
57  
58  
59

**Supplementary Figure 4: CRISPR/Cas9-mediate knockout of mir-615-3p in RKO cells.**  
 a. Schematic design of CRISPR sgRNAs for knockout of mir-615-3p.  
 b. Sanger sequencing confirmed the small deletions in mir-615 hairpin region, which is crucial for the maturation of miR-615-3p in two independent clonal derived RKO cell lines.



60

61

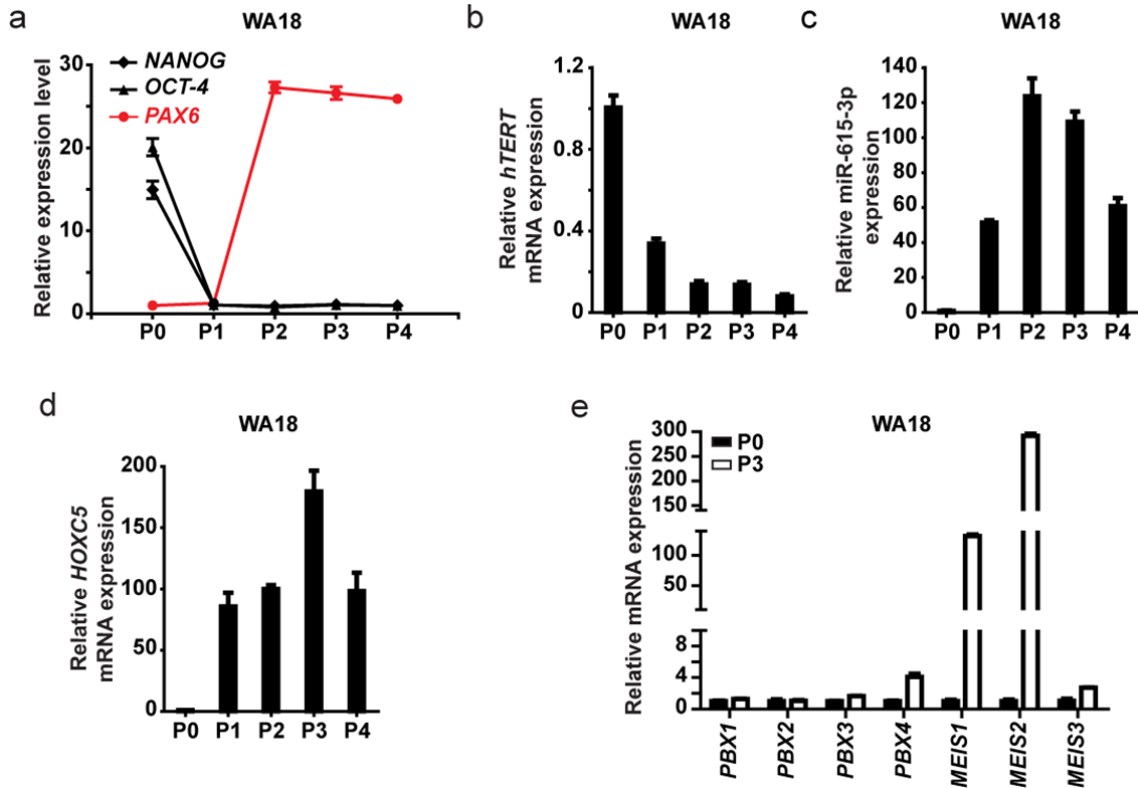
62 **Supplementary Figure 5: Mutation of miR-615-3p binding site in the endogenous**  
 63 ***hTERT* 3'UTR resulted in increased *hTERT* mRNA expression.**

64 a. Relative *hTERT* mRNA expression in parental RKO cells or clonal derived RKO cell lines  
 65 with small deletions or mutations in the *hTERT* 3'UTR. Significance was determined by t-test.  
 66 \*  $P < 0.05$ .

67 b. Sanger sequencing confirmed the small deletions and mutations in *hTERT* 3'UTR region.  
 68 The seed region and the additional conserved site are highlighted in red. The mutated bases  
 69 are highlighted in green.

70 c. Real-time RT-PCR showing the expression of endogenous *HOXC5* mRNA in parental and  
 71 *mir-615-3p* knockout RKO cell lines.

72 d. Western blotting showing the expression of endogenous HoxC5 in parental and *mir-615-*  
 73 *3p* knockout RKO cell lines.



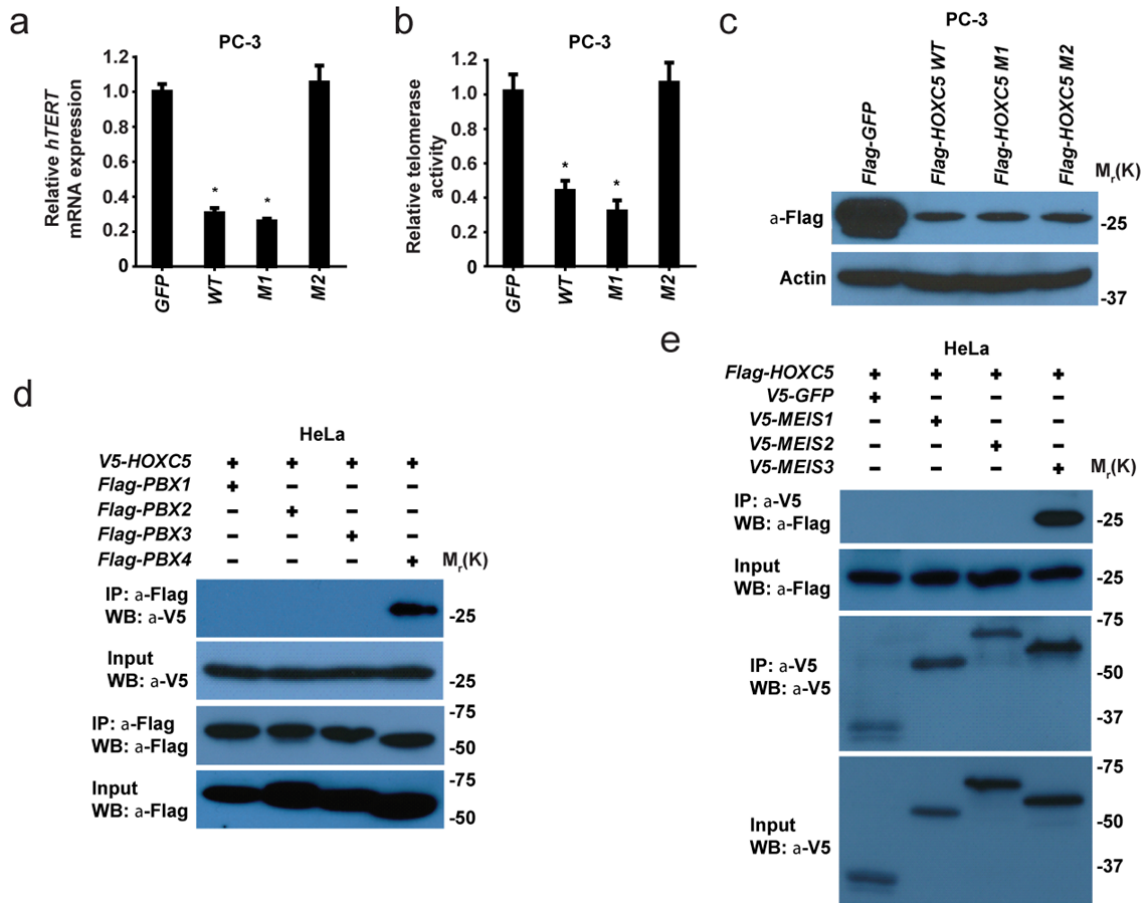
74  
75  
76  
77  
78  
79  
80  
81  
82  
83  
84  
85  
86  
87  
88  
89  
90  
91  
92  
93  
94  
95  
96  
97

**Supplementary Figure 6: Expression of *hTERT*, miR-615-3p, *HOXC5*, *PBX1-4*, and *MEIS1-3* in WA18 human ES cells upon neural induction.**

a. The expression of pluripotency genes (*NANOG* and *OCT-4*) and neurodevelopmental gene *PAX6* during neural differentiation (passage 0 to 4) in WA18 ES cells were quantified by real-time RT-PCR.

b. c. and d. The expression of *hTERT* mRNA, miR-615-3p and *HOXC5* mRNA during neural differentiation (passage 0 to 4) in WA18 cells was quantified by real-time RT-PCR as indicated.

e. The expression of *PBX1-4* and *MEIS1-3* in P0 and P3 of WA18 neural differentiation was quantified by real-time RT-PCR as indicated.



98

99

100

101 **Supplementary Figure 7: HoxC5 recruits Pbx4 and Meis3 to suppress *hTERT***  
 102 **expression.**

103 a. Relative *hTERT* mRNA expression in PC-3 cells transduced with lentivirus overexpressing  
 104 Flag-tagged GFP, wild-type (WT), or mutant (M1 or M2) *HOXC5*. Significance was  
 105 determined by t-test. \*  $P \leq 0.05$ .

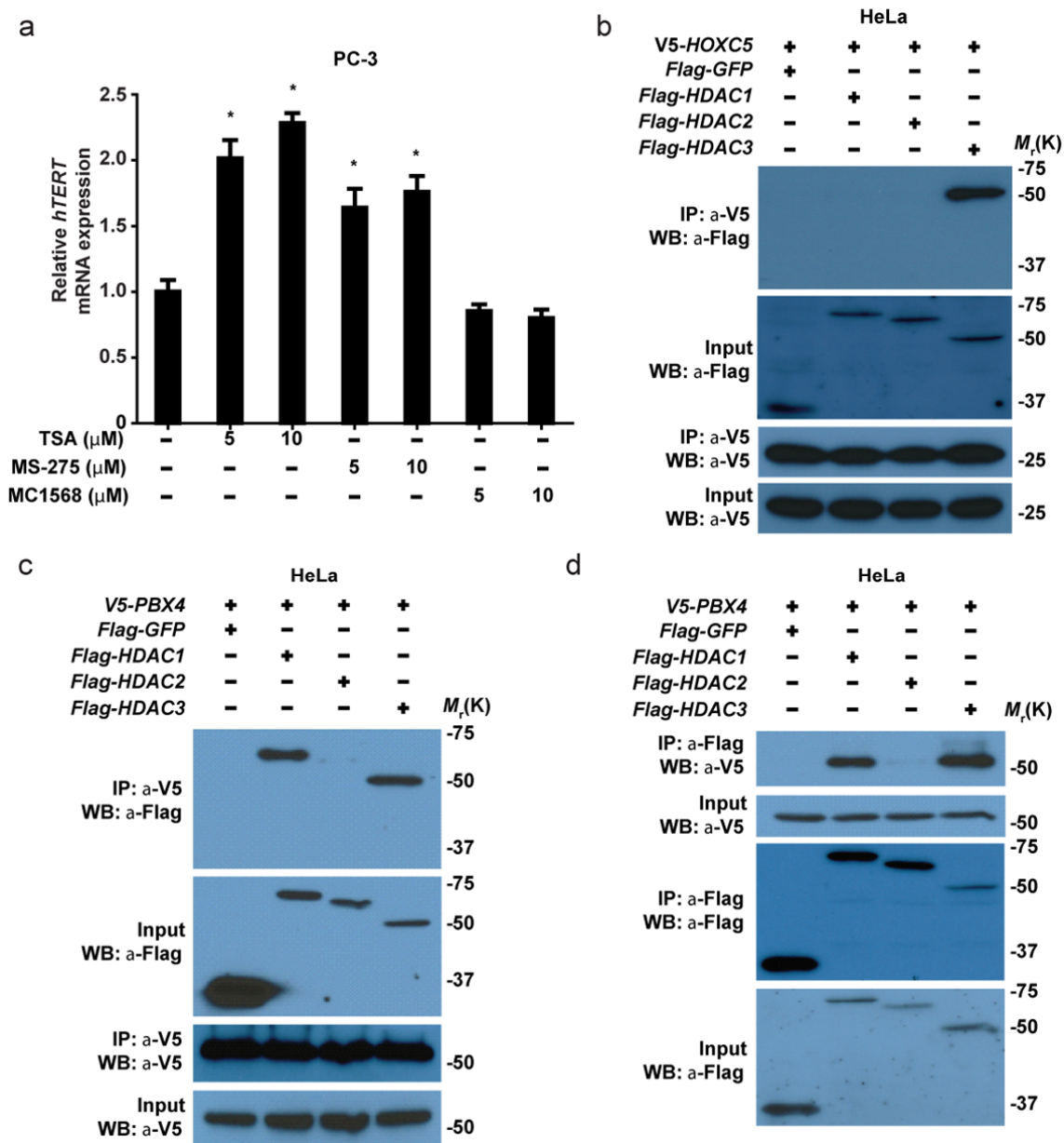
106 b. Relative telomerase activity in PC-3 cells transduced with lentivirus overexpressing Flag-  
 107 tagged GFP, wild-type (WT), or mutant (M1 or M2) *HOXC5*. Significance was determined by  
 108 t-test. \*  $P \leq 0.05$ .

109 c. Western blotting shows the expression of Flag-tagged GFP, wild-type (WT) and mutant  
 110 (M1 or M2) HoxC5 expressed in PC-3 cells.

111 d. Immunoprecipitation of Flag-tagged Pbx4, but not Flag-tagged Pbx1, 2 or 3 resulted in  
 112 specific co-immunoprecipitation of V5-tagged HoxC5 in HeLa cells.

113 e. Immunoprecipitation of V5-tagged Meis3, but not V5-tagged Meis1 or 2 resulted in  
 114 specific co-immunoprecipitation of Flag-tagged HoxC5 in HeLa cells.

115



116

117

118 **Supplementary Figure 8: HDAC1 and 3 containing co-repressor complex is necessary**  
 119 **for HoxC5-Pbx4 mediated suppression of *hTERT* expression.**

120 a. The expression of *hTERT* mRNA in PC-3 cells treated with HDAC inhibitors TSA, MS-275  
 121 or MC1568 as quantified by real-time RT-PCR. Significance was determined by t-test. \*  $P \leq$   
 122 0.05.

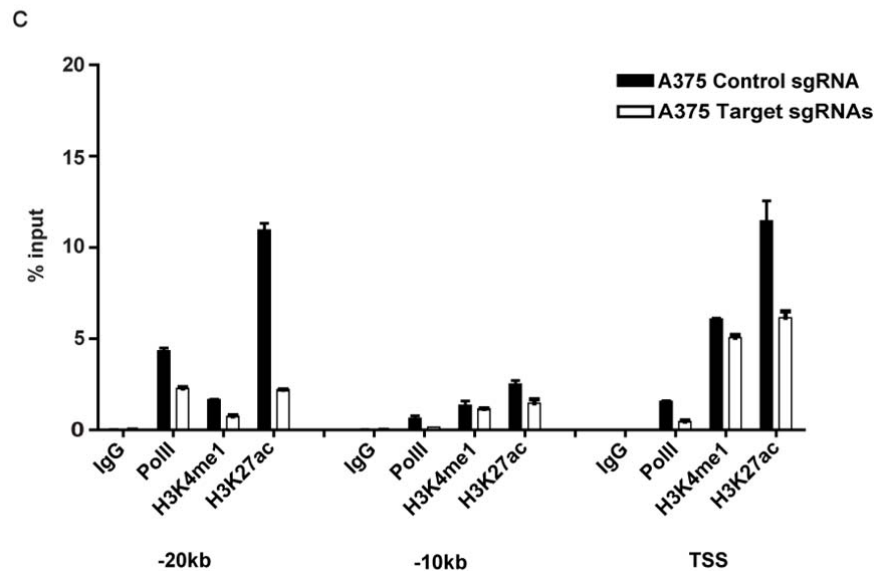
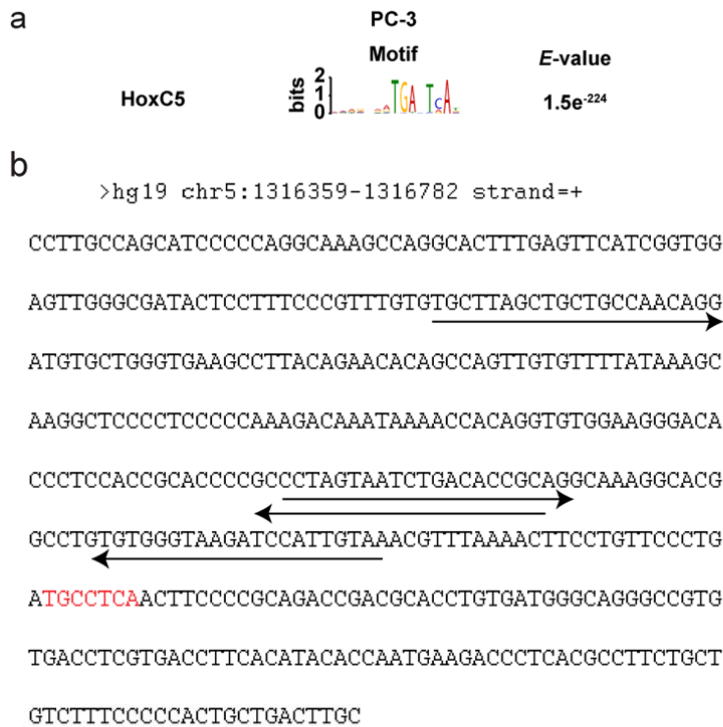
123 b. Immunoprecipitation of V5-tagged HoxC5 resulted in co-immunoprecipitation of Flag-  
 124 tagged HDAC3, but not Flag-tagged HDAC1 or 2 in HeLa cells.

125 c. Immunoprecipitation of V5-tagged Pbx4 resulted in specific co-immunoprecipitation of  
 126 Flag-tagged HDAC1 and 3, but not HDAC2 in HeLa cells.

127 d. Immunoprecipitation of Flag-tagged HDAC1 and 3, but not HDAC2, resulted in efficient  
 128 co-immunoprecipitation of V5-tagged Pbx4 in HeLa cells.

129

130



131

132

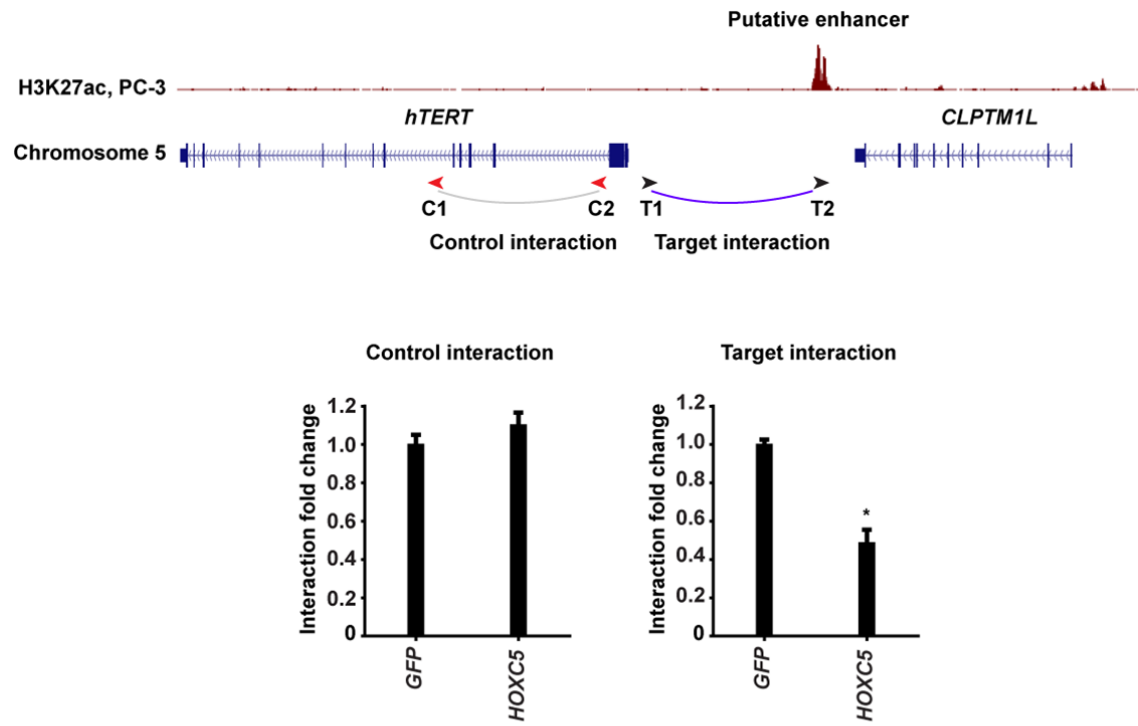
133 **Supplementary Figure 9: Identification of HoxC5 DNA binding motif in *hTERT***  
 134 **upstream enhancer region.**

135 a. The consensus DNA binding motif of HoxC5 was detected using MEME on the  
 136 endogenous HoxC5 binding sites in PC-3 cells.

137 b. The putative binding motif in the *hTERT* -20 kb upstream HoxC5 binding region is  
 138 highlighted in red. The four sgRNAs used in CRISPRi experiment are indicated by arrows.

139 c. ChIP was performed against RNA polymerase II (Pol2), H3K4me1, and H3K27ac in A375  
 140 cells co-expressing dCas9-KRAB with control sgRNA or sgRNAs targeting the HoxC5  
 141 binding region at upstream *hTERT* enhancer followed by qPCR with primers specific for  
 142 *hTERT* TSS, -10kb and -20kb upstream regions as indicated.

143



PC-3

144

145

146 **Supplementary Figure 10: Overexpression of *HOXC5* in PC-3 cells disrupts the long-range interaction between *hTERT* promoter and distal enhancer.** Control interaction:  
 147 Based on the 4C-seq data, we selected a region in the *hTERT* coding region with background levels of interaction, with a similar genomic distance from the *hTERT* bait region  
 148 to serve as a control interaction. Target interaction: long-range interaction between *hTERT* promoter and putative enhancer. Significance was determined by t-test. \*  $P \leq 0.05$ .

151

152

153

154

155

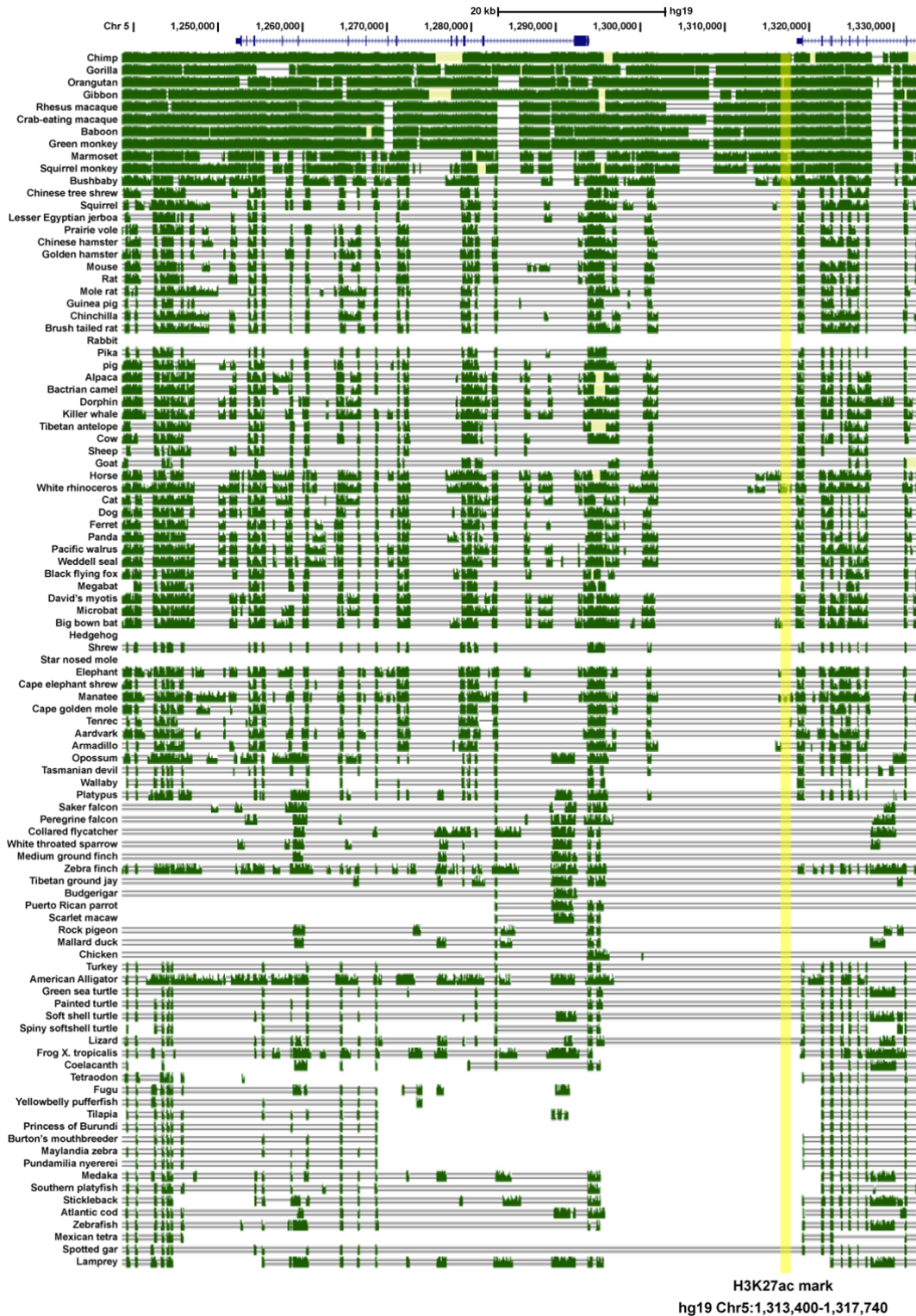
156

157

158

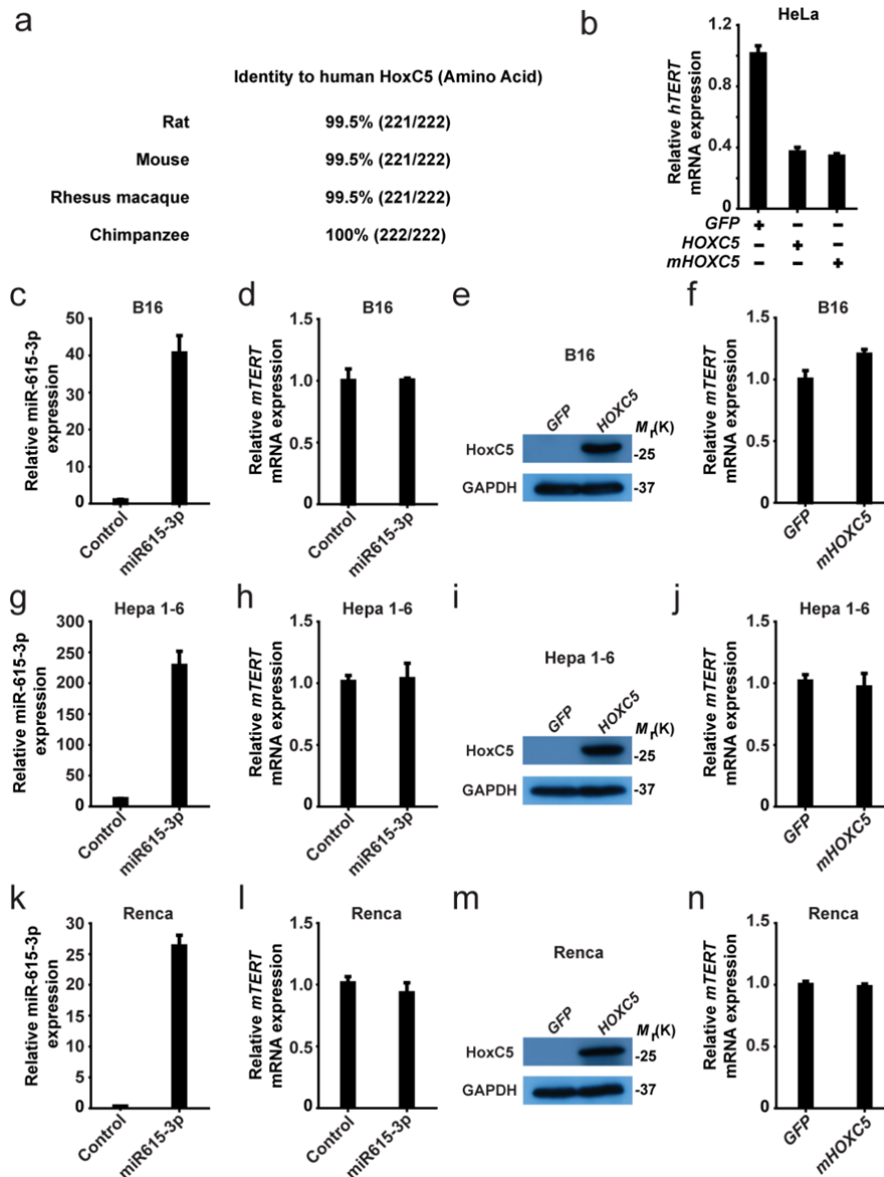
159

160



161

162 **Supplementary Figure 11: The conservation of *hTERT* upstream enhancer region in**  
 163 **100 vertebrate species.** Pairwise alignments of each species to the human genome are  
 164 displayed as histogram to indicate conservation score. The upstream enhancer region is  
 165 highlighted in yellow.



166

167 **Supplementary Figure 12: Distinct function of *HOXC5* in regulation of *TERT***  
 168 **expression in human and mouse cells.**

169 a. The identity of HoxC5 protein from different species in comparison to human HoxC5  
 170 protein was indicated.

171 b. Relative *hTERT* mRNA expression in HeLa transduced with lentivirus overexpressing  
 172 Flag-tagged human or mouse *HOXC5*.

173 c. g. and k. Relative miR-615-3p expression in B16, Hepa 1-6 and Renca mouse cells  
 174 transduced with control lentivirus or lentivirus overexpressing miR-615-3p.

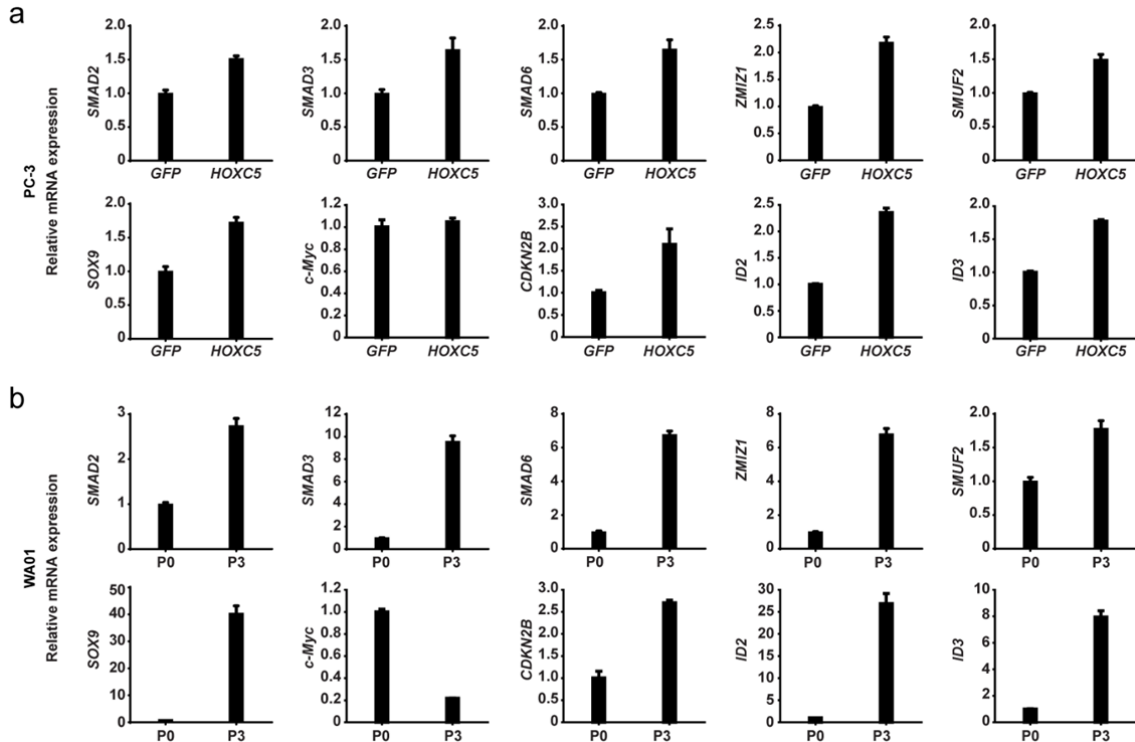
175 d. h. and l. Relative *mTERT* mRNA expression in B16, Hepa 1-6 and Renca mouse cells  
 176 transduced with control lentivirus or lentivirus overexpressing miR-615-3p.

177 e. i. and m. Western blotting showing overexpression of mHoxC5 in B16, Hepa 1-6 and  
 178 Renca mouse cells transduced with control GFP lentivirus or lentivirus overexpressing  
 179 *mHOXC5*.

180 f. j. and n. Relative *mTERT* mRNA expression in B16, Hepa 1-6 and Renca mouse cells  
 181 transduced with control lentivirus or lentivirus overexpressing *mHOXC5*.

182

183

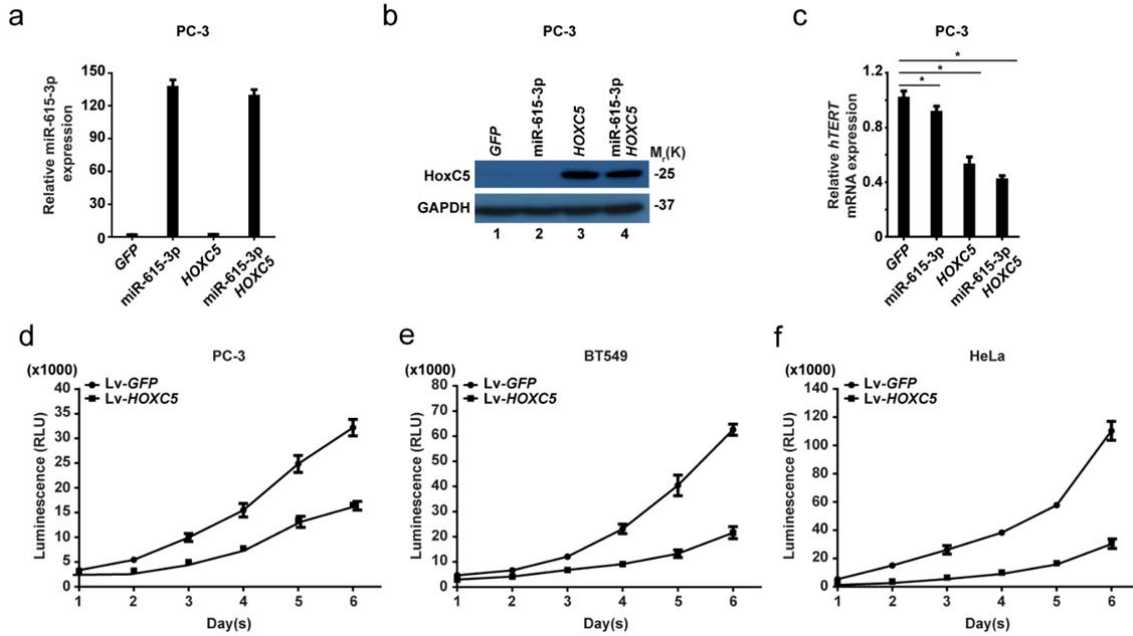


**Supplementary Figure 13: The expression of TGF- $\beta$  target genes**

a. The expression of TGF- $\beta$  target genes in PC-3 cells overexpressing control *GFP* or *HOXC5* was quantified using real-time RT-PCR.

b. The expression of TGF- $\beta$  target genes in human WA01 ES cells before or after neural induction was quantified using real-time RT-PCR.

184  
185  
186  
187  
188  
189  
190  
191  
192  
  
193  
194  
195  
196  
197  
198  
199  
200  
201  
202  
203  
204  
205



206

207

208 **Supplementary Figure 14: Overexpression of *HOXC5* inhibits cancer cell proliferation.**

209 a. Relative expression of miR-615-3p in PC-3 cells that were transduced with lentivirus  
 210 expressing *GFP*, *mir-615-3p*, *Flag-HOXC5* or both *Flag-HOXC5* and *mir-615-3p* as  
 211 quantified using real-time RT-PCR.

212 b. The expression of Flag-tagged HoxC5 in PC-3 cells that were transduced with lentivirus  
 213 expressing *GFP*, *mir-615-3p*, *Flag-HOXC5* or both *Flag-HOXC5* and *mir-615-3p* as shown  
 214 by Western blotting.

215 c. Relative expression of *hTERT* mRNA in PC-3 cells that were transduced with lentivirus  
 216 expressing *GFP*, *mir-615-3p*, *Flag-HOXC5* or both *Flag-HOXC5* and *mir-615-3p* as  
 217 quantified using real-time RT-PCR. Significance was determined by t-test. \*  $P \leq 0.05$ .

218 d. e. and f. Overexpression of *HOXC5*, but not *GFP* inhibits PC-3, BT549 and HeLa cancer  
 219 cells' proliferation as shown by CellTiter-Glo luminescent cell viability assay.

220

221

222

223

224

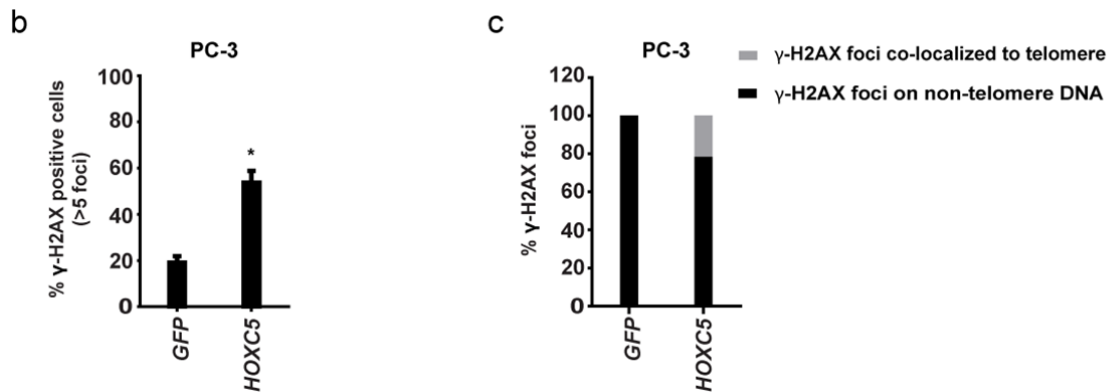
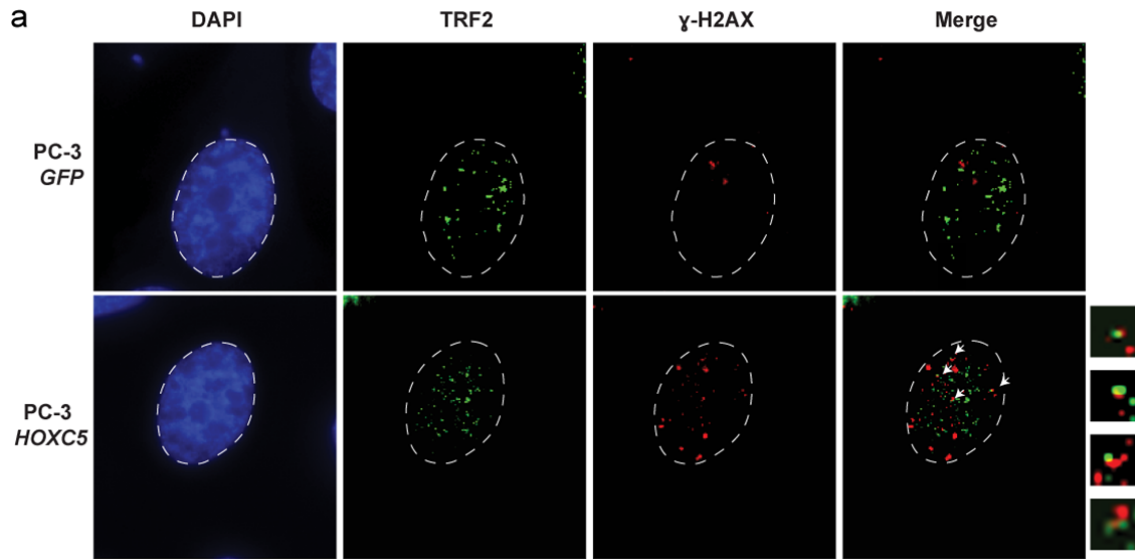
225

226

227

228

229



230

231

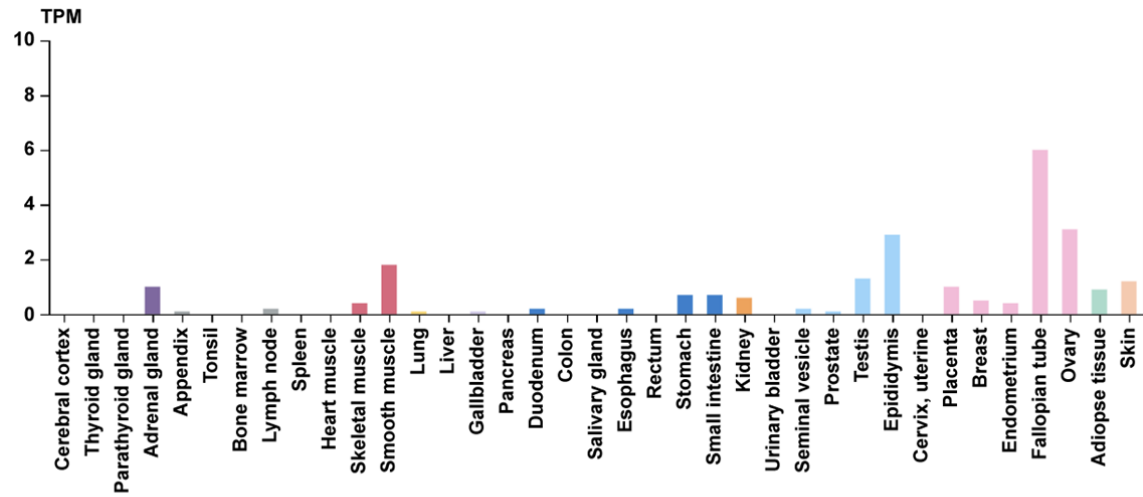
232 **Supplementary Figure 15: Detection of telomere dysfunction-induced foci (TIF) in PC-**  
 233 **3 cells overexpressing HOXC5.**

234 a. Overexpression of *HOXC5*, but not *GFP* in PC-3 cells induced telomeric localization of  $\gamma$ -  
 235 H2AX. Cells were processed for DNA staining (DAPI, blue) as well as double  
 236 immunostaining of TRF2 (green) and  $\gamma$ -H2AX (red). Colocalization of TRF2 and  $\gamma$ -H2AX is  
 237 indicated by arrow and showed in enlarged pictures.

238 b. Comparison of  $\gamma$ -H2AX-positive cells in PC-3 cells overexpressing *GFP* or *HOXC5*. Bars  
 239 represent the mean percentage  $\pm$  SD. Significance was determined by t-test. \*  $P \leq 0.05$ .

240 c. Quantification of  $\gamma$ -H2AX foci detected in a. Signal of  $\gamma$ -H2AX foci overlapping telomeres  
 241 (gray) and those not overlapping (black) are shown separately. A minimum of 100 cells were  
 242 analyzed for each cell line.

243



<http://www.proteinatlas.org/ENSG00000172789-HOXC5/tissue>

244

245

246 **Supplementary Figure 16: Expression of *HOXC5* mRNA in human tissues.**

247

248

249

250

251

252

253

254

255

256

257

258

259

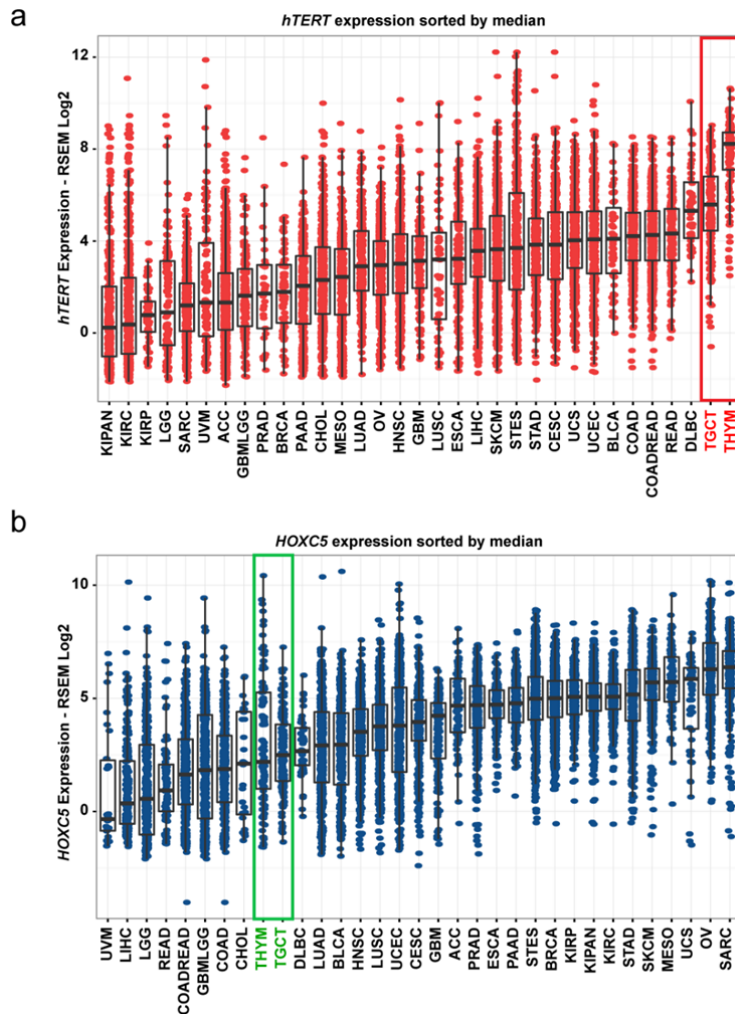
260

261

262

263

264



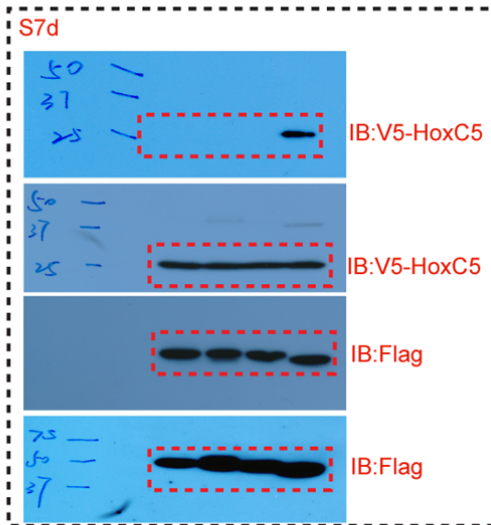
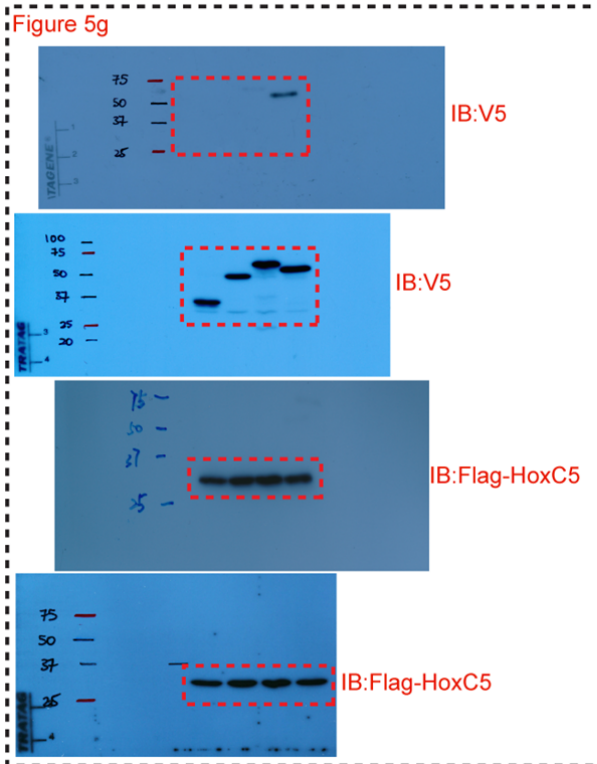
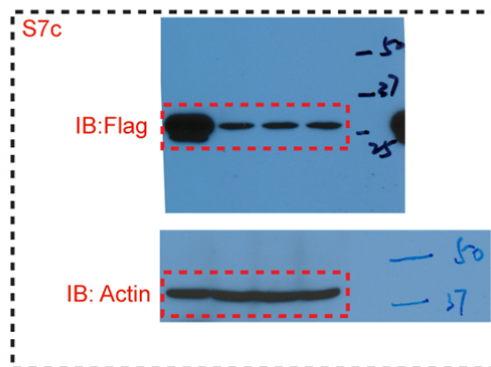
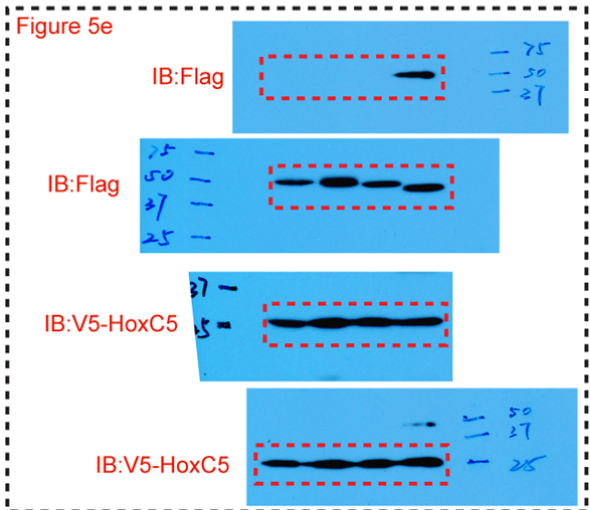
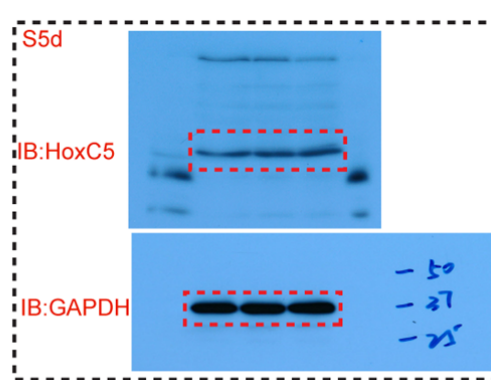
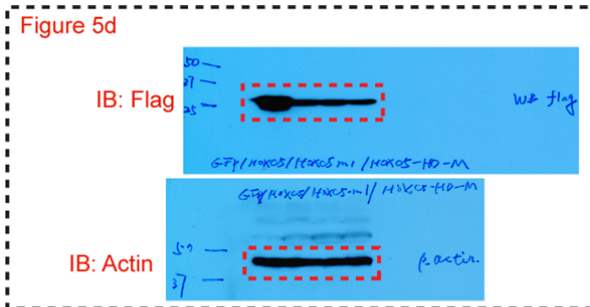
265

266 **Supplementary Figure 17: Expression of *hTERT* and *HOXC5* (Log2 RSEM) in 33**  
 267 **different TCGA cancer types.**

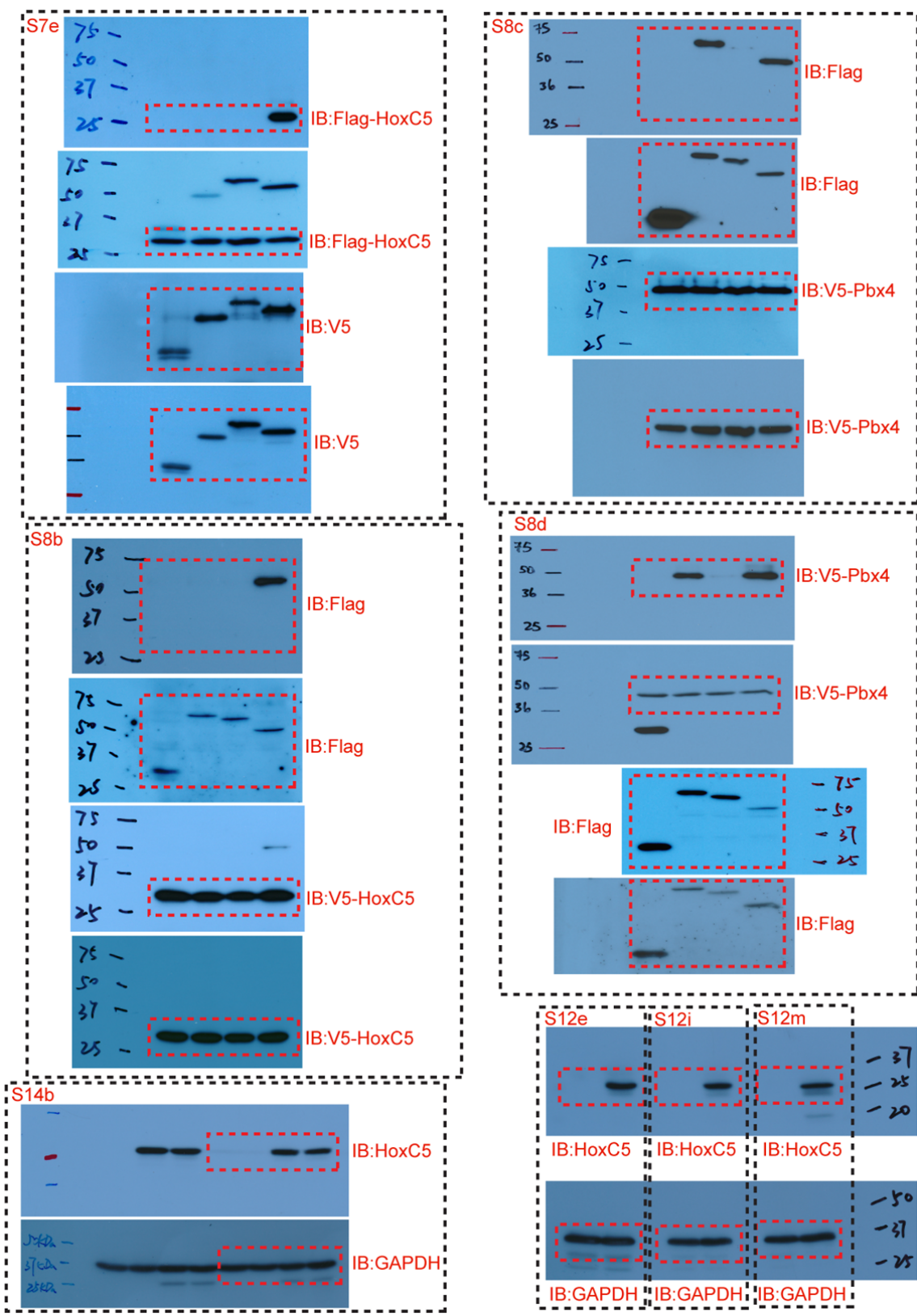
268 a. Boxplot of *hTERT* expression in 33 TCGA cancer types, sorted by median *hTERT*  
 269 expression. TGCT and THYM (highlighted in red box) have the highest median expression  
 270 (5.58 RSEM log2 units for TGCT and 8.23 RSEM log2 units for THYM).

271 b. Boxplot of *HOXC5* expression in 33 TCGA cancer types, sorted by median *HOXC5*  
 272 expression. TGCT and THYM (highlighted in green box) have low median expression  
 273 (2.49 for TGCT and 2.19 for THYM).

274 KIPAN: Pan-Kidney Cohort; KIRC: Kidney Renal Clear Cell Carcinoma; KIRP: Kidney Renal  
 275 Papillary Carcinoma; LGG: Brain Lower Grade Glioma; SARC: Sarcoma; UVM: Uveal  
 276 Melanoma; ACC: Adrenocortical Carcinoma; GBMLGG: Glioma; PRAD: Prostate  
 277 Adenocarcinoma; BRCA: Breast invasive carcinoma; PAAD: Pancreatic Adenocarcinoma;  
 278 CHOL: Cholangiocarcinoma; MESO: Mesothelioma; LUAD: Lung Adenocarcinoma; OV:  
 279 Ovarian Serous Cystadenocarcinoma; HNSC: Head and Neck Squamous Cell Carcinoma;  
 280 GBM: Glioblastoma Multiforme; LUSC: Lung Squamous Cell Carcinoma; ESCA: Esophageal  
 281 Carcinoma; LIHC: Liver Hepatocellular Carcinoma; SKCM: Skin Cutaneous Melanoma;  
 282 STES: Stomach and Esophageal Carcinoma; STAD: Stomach Adenocarcinoma; CESC:  
 283 Cervical and Endocervical Cancers; UCS: Uterine Carcinosarcoma; UCEC: Uterine Corpus  
 284 Endometrial Carcinoma; BLCA: Bladder Urothelial Carcinoma; COAD: Colon  
 285 Adenocarcinoma; COADREAD: Colorectal Adenocarcinoma; READ: Rectum  
 286 Adenocarcinoma; DLBC: Lymphoid Neoplasm Diffuse Large B-Cell Lymphoma; TGCT:  
 287 Testicular Germ Cell Tumor; THYM: Thymoma.



288  
289  
290  
291  
292



293  
294

295 **Supplementary Figure 18: The uncropped western blot scans.**

296

**Supplementary Tables**

297

298

**Supplementary Table 1: The potential targets of miR-615-3p predicted using the microT-CDS algorithm.**

299

300

301

Ensembl Gene Id	miRNA name	miTG score	Ensembl Gene Id	
ENSG00000204052 (LRRC73)	hsa-miR-615-3p	0.996363852	LRRC73	Also predicted by Targetscan
ENSG00000149485 (FADS1)	hsa-miR-615-3p	0.991069849	FADS1	Also predicted by Targetscan
ENSG00000120899 (PTK2B)	hsa-miR-615-3p	0.967646448	PTK2B	Also predicted by Targetscan
ENSG00000163701 (IL17RE)	hsa-miR-615-3p	0.960641477	IL17RE	Also predicted by Targetscan
NSG00000204422 (XXbac-BPG32J3.20)	hsa-miR-615-3p	0.950346894	XXbac-BPG32J3.20	Also predicted by Targetscan
ENSG00000141665 (FBXO15)	hsa-miR-615-3p	0.948559866	FBXO15	Also predicted by Targetscan
ENSG00000204427 (ABHD16A)	hsa-miR-615-3p	0.948532097	ABHD16A	Also predicted by Targetscan
ENSG00000186104 (CYP2R1)	hsa-miR-615-3p	0.942345735	CYP2R1	Also predicted by Targetscan
ENSG00000068305 (MEF2A)	hsa-miR-615-3p	0.940511833	MEF2A	Also predicted by Targetscan
ENSG00000099330 (OCEL1)	hsa-miR-615-3p	0.932861434	OCEL1	Also predicted by Targetscan
ENSG00000153367 (PPM1J)	hsa-miR-615-3p	0.918537497	PPM1J	Also predicted by Targetscan
ENSG00000168488 (ATXN2L)	hsa-miR-615-3p	0.905164923	ATXN2L	Also predicted by Targetscan
ENSG00000103222 (NISCH)	hsa-miR-615-3p	0.903871908	NISCH	Also predicted by Targetscan
ENSG00000162650 (ATXN7L2)	hsa-miR-615-3p	0.900254306	ATXN7L2	Also predicted by Targetscan
ENSG00000196683 (TOMM7)	hsa-miR-615-3p	0.896126765	TOMM7	Also predicted by Targetscan
ENSG00000114857 (NKTR)	hsa-miR-615-3p	0.891295434	NKTR	Also predicted by Targetscan
ENSG00000264058 (KRT222)	hsa-miR-615-3p	0.87832565	KRT222	Also predicted by Targetscan
ENSG00000125304 (TM9SF2)	hsa-miR-615-3p	0.870107894	TM9SF2	Also predicted by Targetscan
ENSG00000130950 (NUTM2F)	hsa-miR-615-3p	0.868009628	NUTM2F	Also predicted by Targetscan
ENSG00000136014 (USP44)	hsa-miR-615-3p	0.866328459	USP44	Also predicted by Targetscan
ENSG00000166436 (TRIM66)	hsa-miR-615-3p	0.860439158	TRIM66	Also predicted by Targetscan
ENSG00000177627 (C12orf54)	hsa-miR-615-3p	0.859569117	C12orf54	Also predicted by Targetscan
ENSG00000213024 (NUP62)	hsa-miR-615-3p	0.853266206	NUP62	Also predicted by Targetscan
ENSG00000172878 (METAP1D)	hsa-miR-615-3p	0.845137038	METAP1D	Also predicted by Targetscan
ENSG00000090006 (LTBP4)	hsa-miR-615-3p	0.843511571	LTBP4	Also predicted by Targetscan
ENSG00000130208 (APOC1)	hsa-miR-615-3p	0.836413839	APOC1	Also predicted by Targetscan
ENSG00000154146 (NRGN)	hsa-miR-615-3p	0.835987146	NRGN	Also predicted by Targetscan
ENSG00000134014 (ELP3)	hsa-miR-615-3p	0.8359661	ELP3	Also predicted by Targetscan
ENSG00000184368 (MAP7D2)	hsa-miR-615-3p	0.835571226	MAP7D2	Also predicted by Targetscan
ENSG00000108671 (PSMD11)	hsa-miR-615-3p	0.827397667	PSMD11	Also predicted by Targetscan
ENSG00000072778 (ACADVL)	hsa-miR-615-3p	0.823677075	ACADVL	Also predicted by Targetscan
ENSG00000163956 (LRPAP1)	hsa-miR-615-3p	0.823040269	LRPAP1	Also predicted by Targetscan
ENSG00000106012 (IQCE)	hsa-miR-615-3p	0.81064738	IQCE	Also predicted by Targetscan
ENSG00000219200 (RNASEK)	hsa-miR-615-3p	0.808783768	RNASEK	Also predicted by Targetscan
ENSG00000173171 (MTX1)	hsa-miR-615-3p	0.80098187	MTX1	Also predicted by Targetscan
ENSG00000105737 (GRIK5)	hsa-miR-615-3p	0.798594078	GRIK5	Also predicted by Targetscan
ENSG00000135003 (POLR3B)	hsa-miR-615-3p	0.791981561	POLR3B	Also predicted by Targetscan
ENSG00000186868 (MAPT)	hsa-miR-615-3p	0.787900988	MAPT	Also predicted by Targetscan
ENSG00000175203 (DCTN2)	hsa-miR-615-3p	0.786717445	DCTN2	Also predicted by Targetscan
ENSG00000179057 (IGSF22)	hsa-miR-615-3p	0.783672468	IGSF22	Also predicted by Targetscan
ENSG00000188171 (ZNF626)	hsa-miR-615-3p	0.782953458	ZNF626	Also predicted by Targetscan
ENSG00000167858 (TEKT1)	hsa-miR-615-3p	0.773304055	TEKT1	Also predicted by Targetscan
ENSG00000135441 (BLOC1S1)	hsa-miR-615-3p	0.771625171	BLOC1S1	Also predicted by Targetscan
ENSG00000179133 (C10orf67)	hsa-miR-615-3p	0.769947324	C10orf67	Also predicted by Targetscan
ENSG00000139567 (ACVRL1)	hsa-miR-615-3p	0.766832637	ACVRL1	Also predicted by Targetscan
ENSG00000132155 (RAF1)	hsa-miR-615-3p	0.766538016	RAF1	Also predicted by Targetscan
ENSG00000163803 (PLB1)	hsa-miR-615-3p	0.764041997	PLB1	Also predicted by Targetscan
ENSG00000102312 (PORCN)	hsa-miR-615-3p	0.763990626	PORCN	Also predicted by Targetscan
ENSG00000143164 (DCAF6)	hsa-miR-615-3p	0.757564443	DCAF6	Also predicted by Targetscan
ENSG00000187486 (KCNJ11)	hsa-miR-615-3p	0.754144971	KCNJ11	Also predicted by Targetscan
ENSG00000168487 (BMP1)	hsa-miR-615-3p	0.752624187	BMP1	Also predicted by Targetscan
ENSG00000182504 (CEP97)	hsa-miR-615-3p	0.749143701	CEP97	Also predicted by Targetscan
ENSG00000130055 (GDPD2)	hsa-miR-615-3p	0.747628184	GDPD2	Also predicted by Targetscan
ENSG00000072071 (LPHN1)	hsa-miR-615-3p	0.734297485	LPHN1	Also predicted by Targetscan
ENSG00000101577 (LPIN2)	hsa-miR-615-3p	0.72952031	LPIN2	Also predicted by Targetscan
ENSG00000185033 (SEMA4B)	hsa-miR-615-3p	0.719097546	SEMA4B	Also predicted by Targetscan
ENSG00000170310 (STX8)	hsa-miR-615-3p	0.713477468	STX8	
ENSG00000187147 (RNF220)	hsa-miR-615-3p	0.704806453	RNF220	
ENSG00000115207 (GTF3C2)	hsa-miR-615-3p	0.702925014	GTF3C2	

302

303

304

305

306

307

308

309

310

311

312

313

314

315

316

Experimentally verified

317 **Supplementary Table 2: Primer sequences for 3C experiments.**

318

319

320

<b>Name</b>	<b>Sequence</b>
Control interaction primer C1	CGGTCGTAGGGTCTGATGTG
Control interaction primer C2	GTCCTCCTGTCTCCATCGTC
Target interaction T1	GTTATTAAGCCAGGCTCAGACT
Target interaction T2	CCGCCCTAGTAATCTGACAC
loading control RP	AGTCCCGCACGCTCATCTT
loading control FP	ACCAAGAAGTTCATCTCCCTGG

321

322

323

324